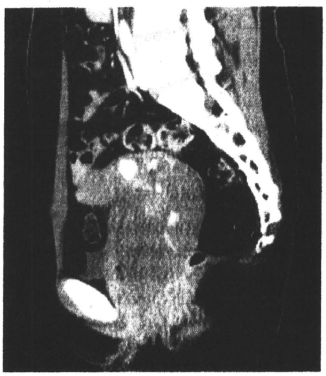

図５　入院後　緊急造影 CT（矢状断）

図６　入院後　3D-CT（後日再構築）

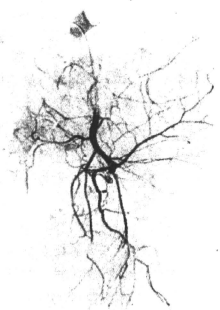

図７　入院後　選択的内腸骨動脈造影
（塞栓術前）

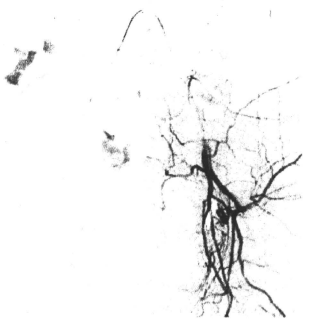

図８　入院後　選択的内腸骨動脈造影
（塞栓術後）

脈塞栓術または子宮全摘術を患者に提示したところ，妊孕性温存希望から前者を選択した．濃厚赤血球４単位の輸血を施行しながら，選択的子宮動脈造影で栄養血管を確定した後（図７），マイクロカテーテル・ゼラチンスポンジを用いた動脈塞栓術を施行．速やかに止血を得た（図８）．施行後の出血は認めず，術後４日目に退院した．その後の外来定期受診においても，出血や異常所見を認めていない．

考　　察

内膜・中膜・外膜に覆われた真性動脈瘤に対して，本来の血管壁に覆われていない動脈瘤を仮性動脈瘤と総称する．外壁は主に結合織で構成されていることが多く，手術や外傷などによる血管損傷・感染・炎症を原因として動脈壁の裂傷が不完全に閉鎖された結果と

して生じる[1]．子宮仮性動脈瘤は非常に稀な疾患であり，文献上も多くは1例報告であるが[2]，傾向として原因となる手術として帝王切開術・D&C・筋腫核出術・子宮全摘術などがあげられ，発症年齢は平均32～34歳，不正性器出血を主訴としている．診断法として確立しているのは経腟エコー・造影CT・血管造影[3]であり，治療法として動脈塞栓術・外科的手術（主に子宮全摘術）があげられる．選択的子宮動脈塞栓術とは，セルジンガー法で大腿動脈からカテーテルを挿入し，骨盤動脈・内腸骨動脈・子宮動脈造影で出血源を同定し，出血源の動脈をゼラチンスポンジ・金属コイル・NBCAなどで塞栓する方法である．分娩後出血での成功率は85～100％程度と報告されていて，術後の妊娠の安全性についても一定の安全性が確立されつつある[4]．本症例は帝王切開術後の不正性器出血である点が典型例といえるが，2度にわたり自然に止血を得られたという点で非典型例であったため，早期の診断は困難であり，合計2300gの出血と8単位の輸血を行うことになった．診断方法・治療方法が確立されつつあるため，診断困難は不正性器出血を主訴に入院し，経腟エコー上で血流のある嚢胞を認めた際に，子宮仮性動脈瘤の可能性を念頭におくことが重要であると考えられる．

結　語

不正性器出血の診断には頻度は少ないが，子宮仮性動脈瘤・子宮動静脈奇形などの病態も念頭におくべきであり，それが早期診断治療を可能にする．また，カラードップラーエコー・造影CTで子宮仮性動脈瘤の診断が得られれば，選択的子宮動脈塞栓術が安全性の高い治療法として考慮される．

文　献

1) Takeda A, Kato K, Mori M et al. Late massive uterine hemorrhage caused by ruptured uterine artery pseudoaneurysm after laparoscopic-assisted myomectomy. J Minim Invasire Gynecol 2008 ; 15 : 212-216
2) Asai S, Asada H, Furuya M et al. Pseudoaneurysm of the uterine artery after laparoscopic myomectomy. Fertil Steril 2009 ; 91 : 929. e1-e3
3) Kim YA , Han YH , Jun KC et al. Uterine artery pseudoaneurysm manifesting delayed postabortal bleeding. Fertil Steril 2008 ; 90 : 849. e11-e14
4) 森田宏紀．子宮動脈塞栓術の適応と効果．日産婦誌　2007 ; 59 : N398-N401

症例報告

腹腔鏡用超音波プローブが有用であった卵管間質部妊娠の一例

東京大学医学部附属病院女性診療科・産科
山本直子、廣井久彦、大須賀　穣、平田哲也、藤本晃久、矢野　哲、武谷雄二

Interstitial pregnancy detection with laparoscopic ultrasound probe: A case report

Naoko Yamamoto, Hisahiko Hiroi, Yutaka Osuga, Tetsuya Hirata,
Akihisa Fujimoto, Tetsu Yano, Yuji Taketani
Department of Obstetrics and Gynecology, University of Tokyo

Abstract Interstitial pregnancy is rare, accounting for 2%-4% of ectopic pregnancies. Massive intra-abdominal bleeding from uterine rupture may be fatal, so early detection and treatment are crucial. We report here a case of interstitial pregnancy detected early via laparoscopic surgical ultrasound probe.

The patient, a 39-year-old female, presented at 5 weeks and 2 days of gestation, according to last menses. The initial serum human chorionic gonadotropin level of 2599 mIU/ml climbed to 4498.6 mIU/ml after two days. With a clinical diagnosis of ectopic pregnancy, emergency laparoscopic exploration was performed, disclosing a swollen left uterine cornu. Passage of an ultrasound probe enabled imaging of left cornual implantation and guided surgical extraction of the gestational sac. The limited uterine defect was easily repaired with negligible total blood loss. Laparoscopic diagnosis and treatment of this interstitial pregnancy was thus expedited through the use of an ultrasound probe.

Key words: ectopic pregnancy, interstitial pregnancy, ultrasound probe for laparoscopic surgery

【緒　言】

卵管間質部妊娠は、異所性妊娠の2～4%[1]といわれており、診断に苦慮することが多い。近年異所性妊娠が経腟超音波やヒト絨毛性ゴナドトロピン（human chorionic gonadotropin; hCG）測定技術の発達から早期に診断することが可能となった。卵管間質部妊娠の初期は症状が現れにくいが、破裂すると腹腔内出血によりショック状態を起こしうるため早期の診断、治療が重要である。また、腹腔鏡下手術の機器や技術の向上に伴い、卵管間質部妊娠に対し、開腹手術でなく、腹腔鏡下手術を施行することが増えている。今回我々は腹腔鏡下超音波プローブを用いて早期に診断し、子宮筋層に大きな欠損を与えることなく治療し得た症例を経験したので報告する。

【症　例】

症例：39歳
妊娠歴：3経妊1経産（自然流産2回）
既往歴：29歳時　子宮筋腫核出術
37歳時　選択的帝王切開術
抗SS-A抗体陽性。挙児希望あり当科習慣流産外来にてスクリーニング検査を行った。proteinS低下のため、妊娠反応陽性が判明した時点で低用量アスピリンを内服開始することとしていた。
現病歴：最終月経起算で妊娠4週6日から低用量アスピリン内服を開始し、妊娠5週2日に当院外来を受診した。来院時所見は内診上異常なく、経腟超音波検査で子宮内に胎嚢様所見を認めなかった。内膜の厚さは15.6mmであり、右卵巣に黄体嚢胞が疑われる所見を認めた。採血にて血中hCGは

2599mIU/mlと高値を示した。2日後の再診察時に自覚症状はなく、やはり経腟超音波検査にて子宮内に胎嚢様所見を認めず、ダグラス窩にecho free spaceも認めなかった。hCG値は4498.6mIU/mlとさらに上昇を認め、異所性妊娠の診断で入院、緊急手術を施行することとした。

手術所見としては、子宮は子宮底側よりみて反時計回りに回転し、左卵管角部が付属器と共にダグラス窩方向に落ち込む方向へ偏移しており、腹膜との癒着を認めた。両側卵管卵巣にも膜様の癒着があったが剥離を行い、妊娠組織様の腫大は認めなかった。右卵巣に黄体嚢胞様部位を認め、腹膜にも病変は認めなかった。左の卵管角が右に比較しやや腫大していたため、左卵管間質部妊娠を疑い腹腔鏡用超音波プローブ（ALOKA UST-52109）を使用し子宮の左卵管角付近を観察したところ高輝度の輪状エコーを認めた。卵黄嚢、胎児心拍は認めなかった（図1A, B）。胎嚢と診断し、腹腔鏡用超音波プローブで観察しつつ、子宮内容除去術を施行した。しかし胎嚢に届かず、経腟的なアプローチは無理であると判断し、腹腔鏡下に卵管角切開術を施行することとした。出血量を抑えるため100倍希釈バソプレシンを左卵管角周囲に局注した。モノポーラ電気メスを用いてマーキングし腹腔鏡用超音波プローブにて胎嚢の位置を確認した後、左卵管角の筋層をモノポーラ電気メスにて約2.5cm切開した（図2）。絨毛様組織を認め、これを除去した（図3）。創部はバイポーラで凝固止血し、インジゴ溶液にて子宮内腔を確認した。肉眼的に妊娠組織様物の残存がないことを確認し、2-0ポリグラクチン縫合糸（バイクリル）3針で切開部を単結紮縫合し、癒着防止吸収性バリア（インターシード）にて切開部を被覆し手術終了とした（図4）。手術時間は3時間4分、出血量は少量であった。

図1A　腹腔鏡用超音波プローブを使用し、子宮を観察。左卵管角が右と比較しやや腫大していた。

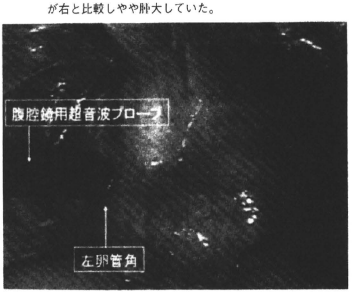

図1B　左卵管角付近にGSを認めた。

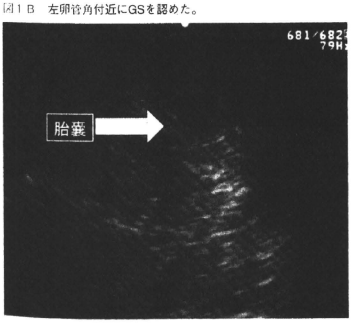

図2　超音波プローブにて確認の後、左卵管角の筋層を切開した。

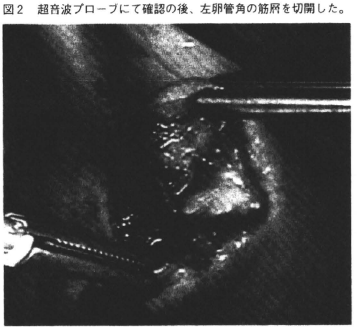

図3　絨毛様組織を認め、除去した。

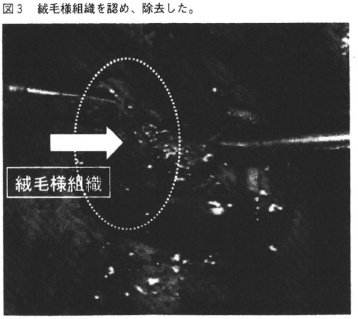

図4　2 0Vicryl 3針で切開部を縫合した。

術後経過は良好であり、術後５日目に退院となった。血中hCGは手術日4498.6mIU/mlであったが、４日後341.7mIU/ml、12日後22.2mIU/ml、19日後3.5mIU/mlと順調に低下した。不正出血もなく、月経は再開し、術後病理では絨毛組織を確認した。

【考　察】

卵管間質部妊娠は子宮筋層内の近位卵管における異所性妊娠である。頻度は異所性妊娠のうち２～３%と稀ではあるが血流が豊富であり、破裂した際には著明な出血を引き起こし、時には生命をも脅かすことのある疾患である[2,3]。

症状は妊娠４～８週で腹痛として起こりうるが、妊娠16週～20週頃まで症状が現れない場合もある[3,4]。腹痛、無月経または妊娠反応陽性の主訴で来院し、子宮内に胎嚢を認めず妊娠反応陽性の時点で異所性妊娠の可能性を考慮する。血中hCGが2000mIU/ml以上であった場合51例中17例は正常妊娠であったという報告もあり[5]、経過観察を行いhCGの上昇によって異所性妊娠を診断すべきである。正常妊娠においては２日（1.2～2.2日）でhCGが約２倍になる[1]。異所性妊娠のうち21%は同様の増加率であるが[6]、多くの例では２倍となるまでにより長い時間がかかり、２日間で1.6倍以下の増加率を認め、低下を認めず、かつ超音波にて子宮内に胎嚢を認めない場合異所性妊娠を強く疑う。ASRM, 2004では、血中hCGについて①48時間で66%以上の上昇でviableと判断。②2400mIU/ml以上のとき、100%経腟超音波で子宮内に胎嚢が確認できる。③子宮内容除去術後にhCG値が15%以上低下を認めない場合異所性妊娠を疑うとしている。本症例では、2599mIU/mlから4498.6mIU/mlと２日で1.73倍の増加を認めており、かつ子宮内に胎嚢を認めないため異所性妊娠が強く疑われた。

経腟超音波検査において卵管間質部妊娠を疑う所見としては、不完全または非対称的な子宮筋層に覆われた胎嚢[7]、子宮内で偏移している胎嚢を認めた場合及び胎嚢が明らかではない場合[8,9]が報告されている。

妊娠部位の診断にCTは有用であると考えられるが、正常妊娠の可能性が否定しきれない場合に使用を躊躇われるため報告例は少ない。CTで未破裂胎嚢を観察した症例報告はこれまで３例、卵管妊娠での報告がある。卵管間質部妊娠に関しては１例の報告があり特徴的所見としては、強く強調された輪状の腫瘤が認められる[10]。MRIもその有用性が報告されており[11]、子宮筋層、子宮内腔に囲まれた位置にGSを認め、junctional zoneを認めた場合強く卵管間質部妊娠が疑われる[12]。緊急時の使用は限られ、費用が高いという側面はあるが、非侵襲的であり本症例でも術前の補助診断に有用であった可能性がある。

腹腔鏡用超音波プローブ（ALOKA UST-52109）は、直径12mm、先端に探触子があり、周波数は３～８MHzである。肝臓、胆嚢の探索などに使われることが多く外科で多用されている。付属器腫瘤の性状の診断を経腟超音波検査と、腹腔鏡用超音波プローブを用いた検査で比較した研究では、的中率が前者では73.5%、後者では83.8%（P<0.05）であり腹腔鏡用超音波プローブを用いた検査がより形態学的詳細の検索に優れていると報告している[13]。腹腔鏡用超音波プローブは、子宮または付属器に直接あてることができるため、距離による減衰の影響をより減少させることができる。また癒着の顕著な症例でも早期の卵管妊娠の部位を正確に診断できる可能性があることが示唆されている[14]。欠点としては、探触子の幅が狭く結果として得られる画像が小さいことが挙げられる。また時間をかけて同部位を観察したい場合には、長細い棒状のプローブの一端を持ち、先端を対象物に対して一定にあてた状態を保持することが求められ、呼吸運動の影響を受けやすい。今回は術中腹腔鏡用超音波プローブを子宮に直接あてることによって、非常に正確に胎嚢の位置を特定することができ、胎嚢の直上の子宮壁を切開して胎嚢を除去することができた。

卵管間質部妊娠の治療は、保存的薬物療法と外科的治療法に分けられる。保存的薬物療法では、

胎芽心拍を認めず、妊孕性温存の希望があり、hCG値も高値ではないなどの条件の場合に適応可能で、メトトレキサートを使用する。しかし、ときに多量の出血を起こすことがあり、薬剤の副作用などの問題もある[9]。また薬物療法が失敗することが予想される状態の一つとして、メトトレキサート投与前に2日間で1.5倍以上のhCG値の上昇を認めた場合が挙げられており[3]、本症例はこれに相当する。本症例では十分な説明を行い、患者が手術療法を選択した。

外科的治療法としてはこれまで子宮角楔状切除術や挙児希望がない場合は単純子宮全摘術を行ってきた。しかし、近年の診断技術の発達により妊娠早期の診断が可能となり卵管角切開術のみで妊娠組織を完全に除去できるようになってきた。今回は腹腔鏡用超音波プローブを用いることにより正確に胎嚢の位置を把握し、切開をその直上においた。約2.5cmの必要最小限の切開創のみで、子宮筋層に欠損を生じず胎嚢を除去し得た。その後3針縫合したのみであり、出血量も少量であった。

卵管間質部妊娠手術療法後の妊娠症例における子宮破裂の可能性については様々な報告がなされている。子宮筋層に欠損があり、特に子宮内膜腔が含まれている場合、子宮破裂の起点となると考えられており[15]縫合によって欠損部位の修復を行えば、子宮破裂のリスクを軽減できると考えられている。また、術中の通電による組織の損傷も子宮破裂の原因となり得ると考えられ、術中使用する機械の電圧や、凝固止血の頻度にも注意が必要である[16]。現時点では、経腟分娩、帝王切開術の選択について統一的見解はなく、個々の症例について検討されているのが実情である。本症例では、線状切開を行っており、子宮筋層の欠損はなく、他に既往がなければこの手術後の妊娠の際には経腟分娩も選択肢の一つであると考えられる。

【結　語】

卵管間質部妊娠は早期の診断、治療が重要である。妊娠早期の症例に対して、腹腔鏡用超音波プローブを用いることにより子宮壁直上からの胎嚢の位置が確認でき、よって最小限の侵襲での治療が可能となった。妊娠早期の卵管間質部妊娠症例において腹腔鏡用超音波プローブの使用は有用であると考える。

本論文の要旨は第49回日本産科婦人科内視鏡学会において発表した。

文　献

1）Levine D.: Ectopic Pregnancy. Radiology 2007; 245: 385-397.
2）William E. et al.: Ruptured Interstitial Pregnancy Presenting as an Intrauterine Pregnancy by Ultrasound. Ann Emerg Med August 1991; 20: 910-912.
3）The Practice Committee of the American Society for Reproductive Medicine.: Medical treatment of ectopic pregnancy. Fertility and Sterility 2008; 90, Suppl3: 206-212.
4）Batzer R.: Guidelines for choosing a pregnancy test. Contemp Obstet Gynecol 1985; 30: 57.
5）Mehta TS et al.: Treatment of ectopic pregnancy: is a human chorionic gonadotropin level of 2,000 mIU/ml a reasonable threshold? Radiology 1997; 205: 569-573.
6）Seeber BE et al.: Suspected ectopic pregnancy. Obstet Gynecol 2006; 107: 399-413.
7）Coady DJ et al.: Ultrasound diagnosis of interstitial pregnancy. NY State J Med 1985; 85: 655-656.
8）Fleischer A.: Ectopic Pregnancy: Features at Transvaginal Sonography. Radiology 1990; 174: 375-378.
9）坂元正一、水野正彦、武谷雄二：卵管間質部妊娠、プリンシプル産科婦人科学、2005；326、メジカルビュー社
10）Shin B: Incidental Detection of Interstitial Pregnancy on CT Imaging. Korean J Radiol 2010; 11: 123-125.
11）Elisabeth Kucera et al.: The Modern Management of Interstitial or Intramural Pregnancy-Is MRI an "Alloyed" Diagnostic Gold Standard or the Real Thing? Fertil Steril 2000; 73: 1063.
12）M.Filhastre et al.: Interstitial pregnancy: role of MRI. Eur Radiol 2005; 15: 93-95.
13）Wei Tse Yang et al.: Intraoperative Laparoscopic Sonography for Improved Preoperative Sonographic Pathologic Characterization of Adnexal Masses. J Ultrasound Med1998; 17: 53-61.
14）D. Grab et al.: Laparoscopic Intraoperative Ultrasound of Adnexal Masses- A pilot Study with 20 Premenopausal Patients. Ultraschall in Med2000; 21: 265-272.
15）Lau S, Tulandi T.: Conservative medical and surgical management of interstitial ectopic pregnancy. Fertil Steril 1999; 72: 207-215.
16）Selma Ng et al.: Laparoscopic management of 53 cases of corneal ectopic pregnancy. Fertil Steril 2009; 92: 448-452.

Human Molecular Genetics, 2010, Vol. 19, No. 3 **480–493**
doi:10.1093/hmg/ddp512
Advance Access published on November 14, 2009

Involvement of a novel preimplantation-specific gene encoding the high mobility group box protein *Hmgpi* in early embryonic development

Mitsutoshi Yamada[1,2], Toshio Hamatani[1,*], Hidenori Akutsu[2], Nana Chikazawa[1,2], Naoaki Kuji[1], Yasunori Yoshimura[1] and Akihiro Umezawa[2]

[1]Department of Obstetrics and Gynecology, Keio University School of Medicine, 35 Shinanomachi Shinjyuku-ku, Tokyo 160-8582, Japan and [2]Department of Reproductive Biology, National Research Institute for Child Health and Development, 2-10-1 Ohkura Setagaya-ku, Tokyo 157-8535, Japan

Received August 24, 2009; Revised October 22, 2009; Accepted November 11, 2009

Mining gene-expression-profiling data identified a novel gene that is specifically expressed in preimplantation embryos. *Hmgpi*, a putative chromosomal protein with two high-mobility-group boxes, is zygotically transcribed during zygotic genome activation, but is not transcribed postimplantation. The *Hmgpi*-encoded protein (HMGPI), first detected at the 4-cell stage, remains highly expressed in pre-implantation embryos. Interestingly, HMGPI is expressed in both the inner cell mass (ICM) and the trophectoderm, and translocated from cytoplasm to nuclei at the blastocyst stage, indicating differential spatial requirements before and after the blastocyst stage. siRNA (siHmgpi)-induced reduction of *Hmgpi* transcript levels caused developmental loss of preimplantation embryos and implantation failures. Furthermore, reduction of *Hmgpi* prevented blastocyst outgrowth leading to generation of embryonic stem cells. The siHmgpi-injected embryos also lost ICM and trophectoderm integrity, demarcated by reduced expressions of Oct4, Nanog and Cdx2. The findings implicated an important role for *Hmgpi* at the earliest stages of mammalian embryonic development.

INTRODUCTION

Preimplantation development encompasses the period from fertilization to implantation. Oocytes cease developing at metaphase of the second meiotic division, when transcription stops and translation is reduced. After fertilization, sperm chromatin is reprogrammed into a functional pronucleus and zygotic genome activation (ZGA) begins, whereby the maternal genetic program governed by maternally stored RNAs and proteins must be switched to the embryonic genetic program governed by *de novo* transcription (1,2). Our previous gene expression profiling during preimplantation development revealed distinctive patterns of maternal RNA degradation and embryonic gene activation, including two major transient 'waves of *de novo* transcription' (3). The first wave during the 1- to 2-cell stage corresponds to ZGA. The second wave during the 4- to 8-cell stage, known as mid-preimplantation gene activation (MGA), induces dramatic morphological changes to the zygote including compaction and blastocele formation, particularly given that few genes show large expression changes after the 8-cell stage. ZGA and MGA together generate a novel gene expression profile that delineates the totipotent state of each blastomere at the cleavage stage of embryogenesis, and these steps are prerequisite for future cell lineage commitments and differentiation. The first such differentiation gives rise to the inner cell mass (ICM), from which embryonic stem (ES) cells are derived, as well as the trophectoderm at the blastocyst stage. However, the molecular regulatory mechanisms underlying this preimplantation development and ES-cell generation from the ICM remain unclear.

Induced pluripotent stem (iPS) cells are ES cell-like pluripotent cells, generated by the forced expression of defined factors in somatic cells, including Pou5f1/Oct4, Sox2, Klf4

*To whom correspondence should be addressed. Tel: +81 353633819; Fax: +81 332261667; Email: t-hama@sc.itc.keio.ac.jp

and Myc (4). These iPS factors are thought to reprogram somatic nuclei in a somewhat similar way as ooplasm does in reconstructed oocytes by nuclear transfer (NT). However, with the exception of Oct4, these factors are not highly expressed maternally in oocytes, and only increased by zygotic transcription during preimplantation, based on expression sequence tag (EST) frequencies in Unigene cDNA libraries and microarray data from oogenesis to preimplantation development (5). Although pluripotency is achieved within 2 days in NT embryos reconstructed with a somatic nucleus, it takes approximately 2 weeks for the establishment of iPS cells. Such immediate induction of pluripotency during preimplantation development is attributed to well-organized transcriptional regulation, i.e. waves of transcription whereby maternal gene products trigger ZGA, which in turn fuels MGA. On the other hand, the forced simultaneous transcription of iPS factors in somatic cells does not efficiently induce these waves of transcription, and it takes a long time to activate the other genes necessary for pluripotency. Studying transcriptional regulation during preimplantation development would therefore also help unravel the establishment of iPS cells as well as pluripotency in these cells.

Large-scale EST projects (6–8) and DNA microarray studies (3,9–11) have revealed many novel genes zygotically expressed during preimplantation development. Very few of these genes, however, are exclusively expressed in preimplantation embryos (12), and such genes ought to have important roles during preimplantation development. For example, *Zscan4*, a novel transcription factor, is expressed specifically in 2-cell stage embryos and a subset of ES cells (13). Reduction of *Zscan4* transcript levels by siRNAs delays progression from the 2-cell to the 4-cell stage, and produces blastocysts that neither implant *in vivo* nor proliferate in blastocyst outgrowth culture. Thus, a transcription factor expressed exclusively in preimplantation embryos is potentially a key regulator of global gene expression changes during preimplantation development. On the other hand, reprogramming gene expression during ZGA and MGA requires considerable changes in chromatin structure (14–16), and modulation of chromatin folding affects access of regulatory factors to their cognate DNA-binding sites. This modulation can be achieved by loosening the chromatin structure, by disrupting the nucleosome structure, by DNA bending and unwinding, and by affecting the strength of DNA-histone interactions via postsynthetic modifications of histones (17,18). Many of these structural changes are mediated by a large and diverse superfamily of high-mobility-group (HMG) proteins, which are the second most abundant chromosomal proteins after histones (18).

This study identified a novel preimplantation-specific gene, *Hmgpi*, which encodes a chromosomal protein containing HMG box domains. It reports a detailed expression analysis of *Hmgpi* and the *Hmgpi*-encoded protein (HMGPI), which was translocated from the cytoplasm to nuclei at the blastocyst stage. Loss-of-function studies were also conducted using siRNA technology. The siRNA-induced reduction in *Hmgpi* expression caused developmental loss at preimplantation stages and hampered implantation through reduced proliferation of both ICM-derived cells and trophectodermal cells during peri-implantation development.

RESULTS

Gene structure of a preimplantation-stage-specific gene, *Hmgpi*

In silico analysis identified *Hmgpi* (an **HMG**-box protein, **pre**implantation-embryo-specific) as a preimplantation-stage-specific gene encoding a chromosomal protein containing HMG box domains. The *Hmgpi* transcript levels are probably upregulated during ZGA (1- to 2-cell stages) to peak at the 4-cell stage, based on gene expression profiling (3,9) (Fig. 1A). Using the public expressed-sequence tag (EST) database, 16 cDNA clones were found exclusively in preimplantation-embryo libraries (2- to 8-cell stages) (Fig. 1B). One of these contained the full *Hmgpi* gene coding sequence (AK163257) (Fig. 1C), spanning 2579 bp and split into two exons, which encode a protein of 394 amino acids (aa) (NP_001028965) harboring a SANT domain ('SWI3, ADA2, N-CoR, and TFIIIB' DNA-binding domain) and two HMG-box domains, based on SMART domain prediction analysis (19) (Fig. 1C). In the NCBI Gene database, the *Hmgpi* gene is called Ubtf-like 1 (*Ubtfl1*) based on aa sequence similarity (36% identity and 58% positives by BLAST) to *Ubtf*-encoded protein 'upstream binding transcription factor', which contains a SANT domain and six HMG-box domains. Two rat homologs (*Ubtfl1* and *RGD1304745*) and three human homologs (*UBTFL1-3*) of the mouse *Hmgpi* were identified by BLASTing of NP_001028965 against the NCBI nucleotide database. Pairwise alignment scores by BLAST of amino acid sequences for rat and human homologs are 72.3–72.5% and 53.8–54.1%, respectively (Fig. 1D and Supplementary Material, Table S1), while those for nucleotide sequences are 83.7 and 66.8–67.0%, respectively. All these human homologs were predicted by *in silico* genome-based analysis, and have no ESTs in the Unigene database. The absence of human ESTs may reflect the paucity of cDNA libraries of human preimplantation embryos in the Unigene database, despite specific expression of the Hmgpi gene in human preimplantation embryos. Based on the number and the type of HMG-box domains, this novel protein could also be categorized into the HMG-box family (HMGB). A dendrogram of aa sequence similarity in HMG family proteins indicates two HMG subgroups (Fig. 1E). One includes the HMG-nucleosome binding family (HMGN) and the HMG-AT-hook family (HMGA), and the other is HMGB that includes HMGPI. All members of HMGB contain two HMG-box domains ('HMG-box' or 'HMG-UBF_HMG-box').

Expression of the *Hmgpi* gene and protein

First, we experimentally confirmed the preimplantaion-stage-specific expression pattern of *Hmgpi* suggested by the *in silico* analysis. Northern blot analysis using a mouse multiple tissue poly(A)RNA panel (FirstChoice® Mouse Blot 1 from Ambion, Austin, TX, USA) failed to detect expression of the *Hmgpi* gene (data not shown). While RT–PCR analysis using cDNA isolated from mouse adult tissues and fetuses (E7, E11, E15 and E17) also failed to show *Hmgpi* expression, RT–PCR analysis for preimplantation embryos indicated *Hmgpi* expression from the 2-cell embryo to the blastocyst

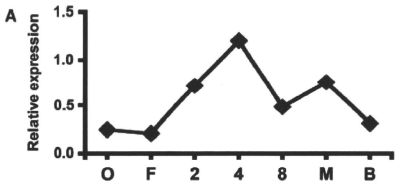

B

Developmental stage	Gene EST	Total EST in pool
Oocyte	0	19488
Unfertilized ovum	0	20366
Zygote	0	28382
Cleavage	16	65852
Blastocyst	0	69936
Egg cylinder	0	12257
Gastrula	0	28673
Organogenesis	0	128591
Fetus	0	670244
Neonate	0	107177
Juvenile	0	293396
Adult	0	1026072

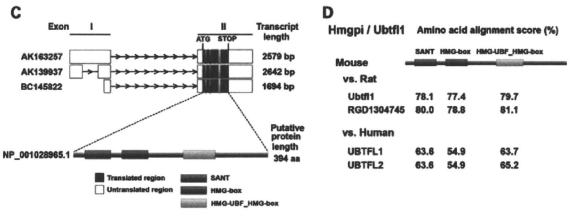

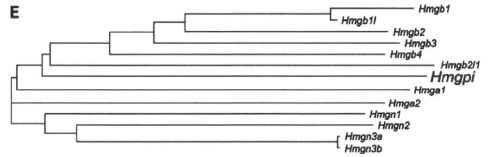

Figure 1. *In silico* analysis of *Hmgpi* expression. (**A**) Previous microarray analysis of *Hmgpi* expression. *Hmgpi* expression appeared at the 2-cell stage, peaked at the 4-cell stage and then decreased (3). (**B**) Expression sequence tag (EST) frequencies in Unigene cDNA libraries. Out of 4.7 million mouse ESTs, 16 *Hmgpi* clones were exclusively detected at the cleavage stages: 9, 2 and 5 ESTs from 2-cell, 4-cell and 8-cell libraries, respectively. (**C**) Exon–intron structures and a putative protein structure of *Hmgpi*. *Hmgpi* has three exon–intron models and one protein model. Predicted protein domains are also shown. (**D**) Conserved domains of *Hmgpi*/*Ubtfl1* gene in mouse, rat and human. Pairwise alignment scores of conserved domains between species were shown. (**E**) Phylogenetic tree of gene nucleotide acid sequences containing HMG domains determined by a sequence distance method and the neighbour-joining (NJ) algorithm (41) using Vector NTI software (Invitrogen, Carlsbad, CA, USA).

stage (Fig. 2A). Furthermore, significant expression of *Hmgpi* was detected in ES cells, although not in embryonic carcinoma (EC) cells nor in mesenchymal stem cells (Fig. 2B). The relative abundance of *Hmgpi* transcripts in preimplantation embryos was measured by real-time quantitative RT–PCR (qRT–PCR) analysis (Fig. 2C). Four independent experiments were conducted with four replicates of 10 embryos each. To normalize the qRT–PCR reaction efficiency, *H2afz* was used as an internal standard (20). *Hmgpi* mRNA levels increased during the 1- to 2-cell stage, peaked at the 4-cell stage, and then gradually decreased during the 8-cell to blastocyst stage (Fig. 2C). The *in silico*-predicted preimplantation-stage-specific expression pattern of *Hmgpi* was therefore validated.

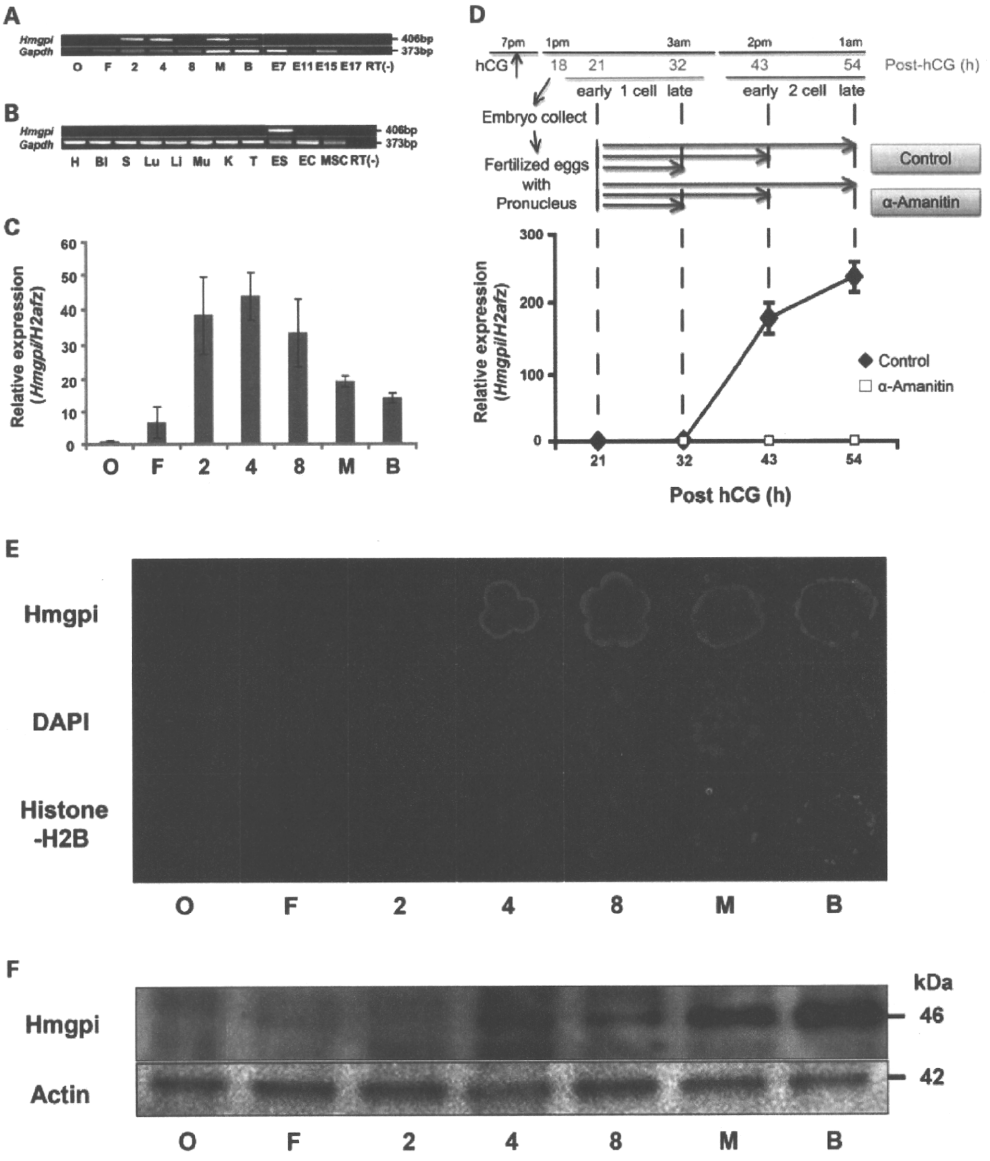

Figure 2. Expression of *Hmgpi* in preimplantation embryos and other tissues. (**A**) RT–PCR analysis of *Hmgpi* expression during preimplantation and postimplantation development (E7–E17). Three sets of 10 pooled embryos were collected from each stage (O: oocyte, F: fertilized egg, 2: 2-cell embryo, 4: 4-cell embryo, 8: 8-cell embryo, M: morula, and B: blastocyst) and used for RT–PCR analysis. The predicted sizes of the PCR products of *Hmgpi* and *Gapdh* are 406 and 373 bp, respectively. No PCR products were detected in the no-RT negative control (4-cell embryo). (**B**) RT–PCR analysis of *Hmgpi* expression in adult tissues, ES cells, EC cells and mesenchymal stem cells. mRNA was isolated from mouse tissues (H: heart, Bl: bladder, S: spleen, Lu: lung, Li: liver, Mu: muscle, K: kidney, T: testis, ES: ES cells, EC: EC cells, and MSC: mesenchymal stem cells). No PCR products were detected in the no-RT negative control (ES cells). (**C**) Real-time quantitative RT–PCR analysis of *Hmgpi* expression during preimplantation development. Fold differences in amounts of *Hmgpi* mRNA from the same numbers of oocytes (O), fertilized eggs (F), 2-cell embryos (2), 4-cell embryos (4), 8-cell embryos (8), morulae (M) and blastocysts (B) are shown after normalization to an internal reference gene (mouse *H2afz*). Values are means ± SE from four separate experiments. (**D**) *De novo* (zygotic) transcription of the *Hmgpi* gene. α-Amanitin studies revealed that *Hmgpi* is transcribed zygotically, but not maternally. *Hmgpi* expression was not observed before the 2-cell stage and α-amanitin completely inhibited *de novo* transcription at the 2-cell stage (closed rhombus: control group, open square: α-amanitin-treated group). The expression levels were normalized using *H2afz* as a reference gene. Values are means ± SE from four separate experiments. (**E**) Immunocytochemical analysis of HMGPI expression. MII oocytes and preimplantation embryos were immunostained with an anti-HMGPI antibody (red) and an anti-Histone-H2B antibody as a positive control of nuclear staining (green). Nuclei are shown by DAPI staining (blue). HMGPI protein was detected from 4-cell embryos to blastocysts. (**F**) Immunoblot analysis of HMGPI during preimplantation development. An amount of extracted protein corresponding to 100 oocytes or embryos was loaded per lane. Actin was used as a loading control. The representative result is shown from three independent experiments.

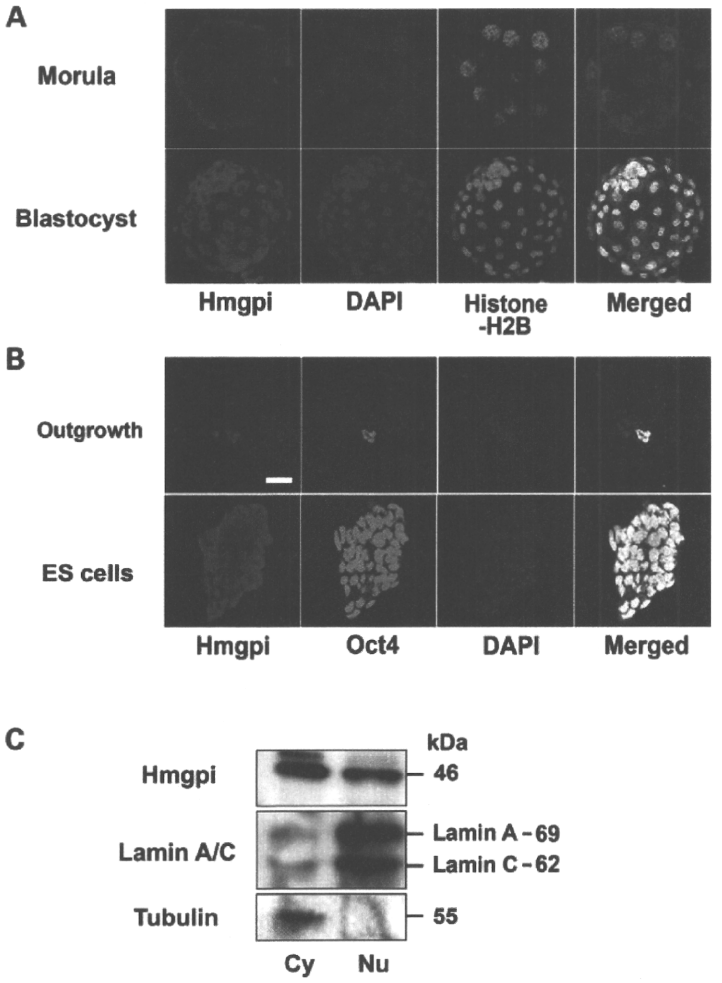

Figure 3. Localization of HMGPI in preimplantation embryos. (**A**) Nuclear translocation of HMGPI protein at the blastocyst stage. HMGPI was mainly detected in the cytoplasm of preimplantation embryos (from 4-cell embryos to morulae), but in the nuclei of blastocysts. Nuclei are shown by immunostaining with an anti-Histone-H2B antibody (green) and DAPI staining (blue). (**B**) Confocal microscopy images of blastocyst outgrowth and ES cells stained with antibodies to *Hmgpi* and *Oct4*, and with DAPI. Scale bar = 50 μM. (**C**) Western blotting analysis of HMGPI in cytoplasmic (Cy) and nuclear (Nu) fractions of ES cells. Lamin A/C and tubulin were used as markers of the nuclear and cytoplasmic fractions, respectively.

We then performed qRT–PCR analysis using α-amanitin to investigate *de novo* (zygotic) transcription of the *Hmgpi* gene. The supplementation of α-amanitin during *in vitro* culture from the 1-cell stage significantly reduced *Hmgpi* mRNA expression in the 2-cell embryos at post-hCG 43 and 53 h (early and late 2-cell stage, respectively) (Fig. 2D), implying that *Hmgpi* is transcribed zygotically during the major burst of ZGA, but not maternally.

To study the temporal and spatial expression pattern of the *Hmgpi*-encoded protein (HMGPI), we raised a polyclonal antibody against *Hmgpi* peptides. Western blot analysis of extracts from the mouse blastocysts showed only a single band corresponding to 46 kDa detected by the anti-HMGPI antibody. In addition, preincubation with the HMGPI peptide antigen abolished detection of the HMGPI protein, while preincubation with a control peptide had no effect on the immunodetection (Supplementary Material, Fig. S1). Although *Hmgpi* transcription started at the 2-cell stage, peaked at the 4-cell stage and then gradually decreased until the blastocyst stage (Fig. 2C), immunostaining and immunoblotting analysis revealed HMGPI expression from the 4-cell stage until the blastocyst stage, indicating a delayed expression pattern of HMGPI compared with that of the *Hmgpi* transcript. It was also notable that both ICM cells and trophectodermal cells retained HMGPI expression in blastocysts.

On the other hand, immunostaining for HMGPI in preimplantation embryos showed a unique subcellular localization pattern. Although a putative nuclear protein due to its role

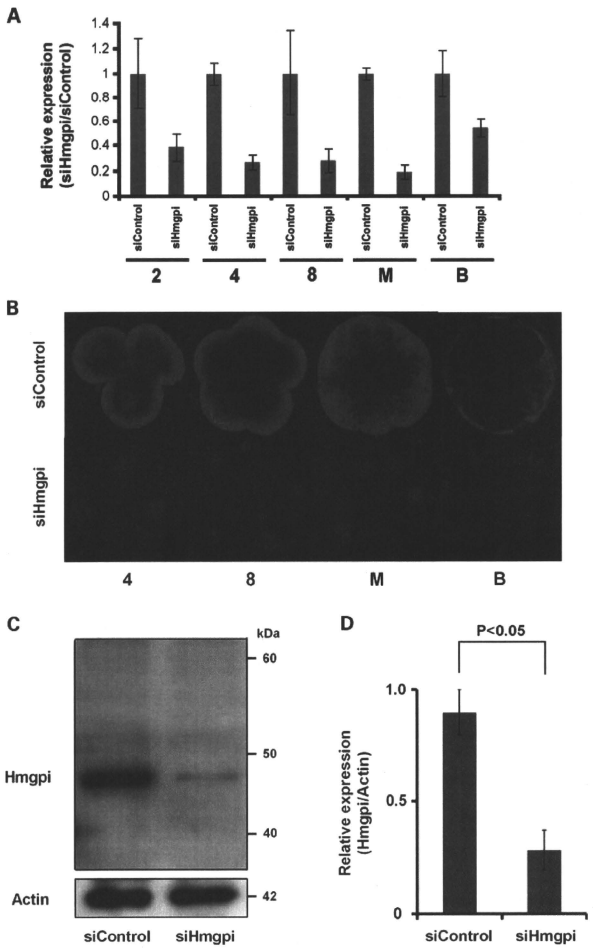

Figure 4. Loss-of-function study by siRNA technology. (**A**) Transcript levels of *Hmgpi* in embryos injected with control siRNA (siControl) and *Hmgpi* siRNA (siHmgpi) by real-time quantitative RT–PCR analysis. The expression levels were normalized using *H2afz* as a reference gene. Values are means ± SE for four separate experiments. (**B**) Laser scanning confocal microscopy images of HMGPI protein expression in a 4-cell embryo, 8-cell embryo, morula and blastocyst after injection with siControl or siHmgpi (red, HMGPI; blue, chromatin). (**C** and **D**) Immunoblot analysis of HMGPI expression at the blastocyst stage in siControl-injected and siHmgpi-injected embryos. The relative amount of HMGPI (46 kDa) was determined at the blastocyst stage (left: siControl-injected embryos, right: siHmgpi-injected embryos). The expression levels were normalized using actin expression (42 kDa) as a reference. Values are means ± SE from three separate experiments.

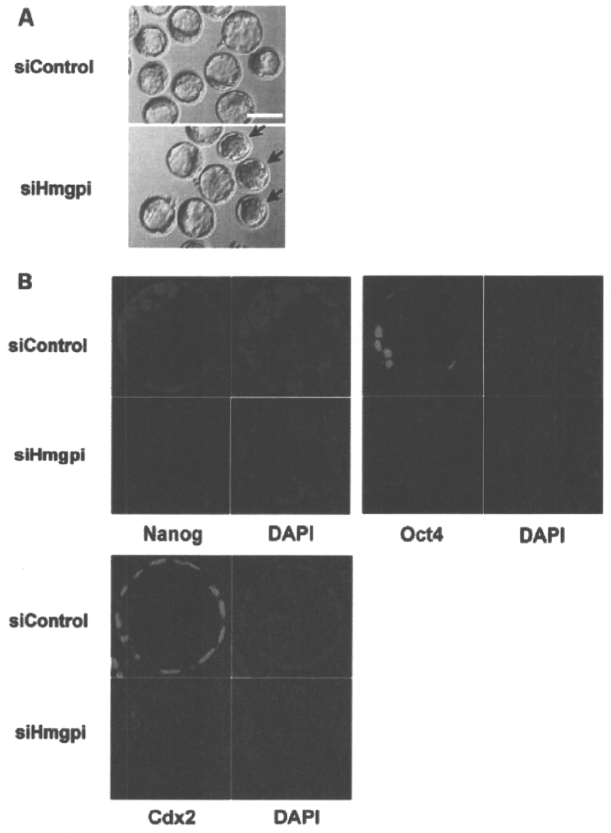

Figure 5. Function of *Hmgpi* in preimplantation development. (**A**) A pair of representative photos showing the development of embryos injected with *Hmgpi* siRNA (siHmgpi) and Control siRNA (siControl). The siHmgpi-injected embryos arrested at the morula stage are indicated by arrows. Scale bar = 100 μM. (**B**) For Nanog, Oct4 and Cdx2 immunostaining, all blastocysts in the siHmgpi-injected and siControl-injected groups were processed simultaneously. The laser power was adjusted so that the signal intensity was below saturation for the developmental stage that displayed the highest intensity and all subsequent images were scanned at that laser power. This allowed us to compare signal intensities for Nanog, Oct4 and Cdx2 expression between the siHmgpi-injected and siControl-injected embryos (Supplementary Material, Table S2).

as a transcription factor, HMGPI was detected mainly in the cytoplasm without any evidence of a nuclear localization from the 4-cell to the morula stage, suggesting a role other than transcriptional regulation (Fig. 2E). In contrast, HMGPI was localized to the nuclei rather than to the cytoplasm of blastocysts (Figs 2E and 3A). During blastocyst outgrowth, HMGPI was expressed in the nuclear region of most outgrowing cells, with scant amounts detected in the cytoplasm (Fig. 3B). Interestingly, Oct4-positive cells derived from the ICM showed particularly strong positive staining for HMGPI in the nucleus, suggesting a specific role as a nuclear protein in ES cells (Fig. 3B). On more closely examining HMGPI in ES cells, we found that almost all the Oct4-positive undifferentiated ES cells in a colony also expressed HMGPI (Fig. 3B), and immunoblotting confirmed HMGPI expression in both nuclear and cytoplasmic fractions of ES cells (Fig. 3C).

Effect of siRNA on *Hmgpi* mRNA level and protein synthesis

To investigate a role of *Hmgpi* in early embryonic development, we knocked down *Hmgpi* expression in mouse preimplantation embryos. We employed an oligonucleotide-based siRNA (denoted here siHmgpi and obtained from PE Applied Biosystems, Foster City, CA, USA). Zygotes injected with *Hmgpi* siRNAs (siHmgpi) or control siRNA (siControl) and non-injected zygotes as negative controls were cultured. *Hmgpi* expression was severely suppressed in the siHmgpi-injected embryos, and significantly lower than those in the siControl-injected or non-injected embryos (Fig. 4A). The siControl-injected embryos did not show any difference from the non-injected embryos in *Hmgpi* expression (data not shown). In addition, immunofluorescent staining clearly demonstrated that the siRNA injection reduced HMGPI protein expression in an individual preimplantation embryo (Fig. 4B). In the same set of experiments, the HMGPI levels were also assayed by western blotting (Figs 4C and 4D). HMGPI expression was significantly reduced in siHmgpi-injected blastocysts (0.89 ± 0.10) compared with that in negative controls (0.28 ± 0.08; $P < 0.05$).

Furthermore, we confirmed that siHmgpi had no influence on the expression of other genes with sequence similarities to *Hmgpi*, namely *Ubtf*, *Hmgb1*, *Hmgb2* and *Hmgb3*. Although *Ubtf*, *Hmgb1*, *Hmgb2* and *Hmgb3* were all expressed in control preimplantation embryos, the siHmgpi construct used in this study did not affect the expression of these genes in the siHmgpi-injected embryos (Supplementary Material, Fig. S2). On the other hand, it has been demonstrated that loss-of-function of these genes produces no distinct phenotypes at the pre- and peri-implantation stages (21).

Effect of *Hmgpi* siRNA on preimplantation development

To study the function of *Hmgpi* during preimplantation development, siHmgpi-injected or siControl-injected zygotes were cultured *in vitro* until the blastocyst stage. The embryos injected with siHmgpi at 21–23 h after hCG administration often failed to become blastocysts at 3.5 days postcoitum (dpc) (Fig. 5A). In addition, the reduction in Hmgpi expression significantly suppressed preimplantation development, whereby $68.9 \pm 1.3\%$ of siHmgpi-injected embryos became blastocysts, while $94.1 \pm 1.3\%$ of siControl-injected embryos reached the blastocyst stage (Supplementary Material, Fig. S3; $P < 0.0001$). Most of the siHmgpi-injected embryos that failed to become blastocysts showed developmental arrest after the morula stage and did not appear to form blastocoels, suggesting impairment of trophectodermal development (Supplementary Material, Fig. S3). To analyze the phenotype of siHmgpi-injected embryos further, we performed immunofluorescence staining of lineage-specific markers such as Cdx2, Nanog and Oct4 at the blastocyst stage. Although siHmgpi-injected embryos that reached the blastocyst stage appeared morphologically intact, the expression of lineage-specific markers was reduced (Fig. 5B). Cdx2, which is required for implantation and extra-embryonic development, was particularly and markedly down-regulated in trophectodermal cells, while Nanog and Oct4

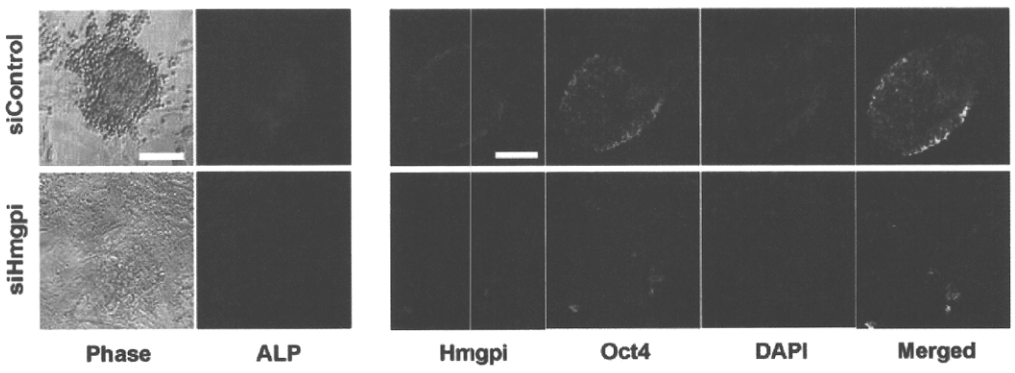

C

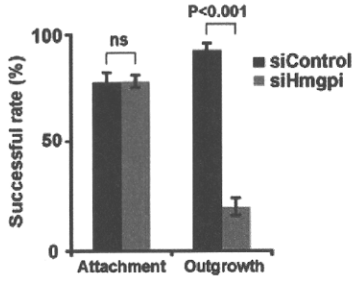

	Tested blastocysts	Attachment (%)	Outgrowth (%)
siControl	51	34 (66.6)	30 (88.2)
siHmgpi	20	15 (75.0)	2 (13.3)
siControl	117	92 (78.6)	80 (86.9)
siHmgpi	13	10 (76.9)	2 (20.0)
siControl	55	49 (89.0)	48 (97.9)
siHmgpi	8	7 (87.5)	1 (14.2)
siControl	41	33 (80.4)	33 (100.0)
siHmgpi	13	10 (76.9)	3 (30.0)

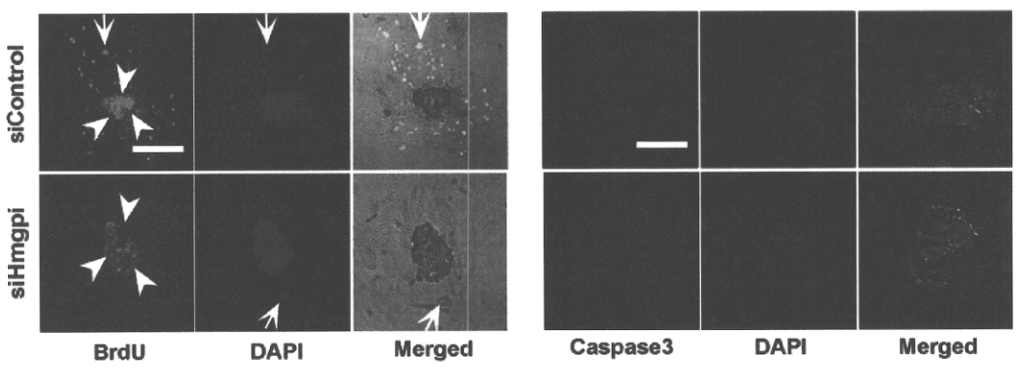

F

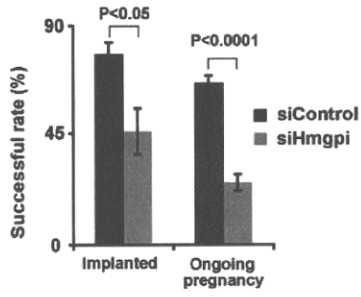

	Transferred embryos	Implanted (%)	Ongoing pregnancy (%)
siControl	30	23 (76.7)	20 (66.7)
siHmgpi	18	6 (33.3)	3 (16.7)
siControl	30	25 (83.3)	18 (60.0)
siHmgpi	32	20 (62.5)	10 (31.2)
siControl	16	13 (81.2)	12 (75.0)
siHmgpi	24	15 (62.5)	7 (29.1)
siControl	20	13 (65.0)	13 (65.0)
siHmgpi	32	8 (25.0)	7 (21.8)

were likewise downregulated in ICM cells of the siHmgpi-injected embryos (Fig. 5B and Supplementary Material, Table S2). Thus, *Hmgpi* is essential for the earliest embryonic development; both ICM and trophectodermal development.

Effect of *Hmgpi* siRNA on *in vivo* and *in vitro* peri-implantation development

To investigate the role of *Hmgpi* in proliferation of the ICM and trophectodermal cells, siHmgpi-injected and siControl-injected embryos were further cultured *in vitro* from the blastocyst stage, and attachment and outgrowth of each embryo on gelatin-coated culture plates was examined. HMGPI expression in siHmgpi-injected embryos was significantly reduced, and immunostaining showed that many colonies of ICM cells in the embryos collapsed during outgrowth culture (Fig. 6A and B). Although the vast majority of ICMs from siControl-injected embryos showed successful attachment (80.3 $\pm$ 4.9%) and vigorous outgrowth (96.2 $\pm$ 2.7%), those from siHmgpi-injected embryos failed to proliferate or produced only a residual mass (19.3 $\pm$ 3.8%) despite successfully attaching (79.0 $\pm$ 2.8%) (Fig. 6C; attachment ns; outgrowth, $P < 0.001$). These results implied that *Hmgpi* is essential for proliferation of ICM and trophectodermal cells in peri-implantation development, and for derivation of ES cells.

We then investigated cell proliferation and apoptosis during blastocyst outgrowth. Comparable incorporation of BrdU in blastocyst outgrowths of siHmgpi-injected embryos was less than that of siControl-injected embryos. Proliferation was significantly reduced in ICM-derived cells and dramatically suppressed in trophoblast cells (Fig. 6D). Embryonic fibroblasts were used as a feeder layer in this study and could support ICM cells, thus proliferation should have proceeded regardless of trophectodermal cell support. Therefore, the collapsed ICM-derived colonies in the current experiment were not a secondary effect of reduced proliferation in trophoblast cells, but a direct effect of the siHmgpi-induced decrease in ICM proliferation. Apoptosis was not detected in any cells during blastocyst outgrowth of siHmgpi-injected embryos, based on the absence of active caspase3 (Fig. 6E). Taken together, these findings show that *Hmgpi* is indispensable for proliferation of the ICM and trophectodermal cells in peri-implantation development and for the generation of ES cells.

Finally, we tested whether the experimental blastocysts could develop *in vivo* by transferring siHmgpi-injected and siControl-injected blastocysts into the uterus of pseudopregnant mice. Only 45.8 $\pm$ 9.7 and 24.7 $\pm$ 3.3% of blastocysts injected with siHmgpi implanted and developed, respectively, whereas most of the siControl-injected embryos showed successful implantation and ongoing development (76.5 $\pm$ 4.0 and 66.6 $\pm$ 3.3%, respectively) (Fig. 6F; implanted, $P < 0.05$; ongoing pregnancy, $P < 0.0001$). These results confirmed a role for *Hmgpi* in peri-implantation embryonic development.

DISCUSSION

We previously analyzed the dynamics of global gene expression changes during mouse preimplantation development (3). Understanding these preimplantation stages is important for both reproductive and stem cell biology. Many genes showing wave-like activation patterns (e.g. ZGA and MGA) during preimplantation were identified, and any or all of these may contribute to the complex gene regulatory networks. *Hmgpi*, one of the few novel preimplantation-specific genes, is involved in early development, implantation and ES cell derivation.

Structure-based prediction of *Hmgpi* function

Structural information about a protein sometimes hints at functional mechanisms, which remain unknown for *Hmgpi*'s clear role in early embryonic development. The HMG family proteins are abundant nuclear proteins that bind to DNA in a non-sequence-specific manner, influence chromatin structure and enhance the accessibility of binding sites to regulatory factors (17). Based on the number and the type of HMG domains, *Hmgpi* is relevant to the HMGB subfamily, characterized by containing two HMG-box domains ('HMG-box' or 'HMG-UBF_HMG-box'), rather than either the HMGA or HMGN subgroups. *Hmgpi* is also known as *Ubtfl1* in the NCBI gene database, based on sequence similarity to *Ubtf*, a well-known ZGA gene (3,22). *Ubtf*, encoding a SANT domain and six HMG-box domains, functions exclusively in RNA polymerase I (Pol I) transcription (23) and acts through its multiple HMG boxes to induce looping of DNA, which creates a nucleosome-like structure to modulate tran-

Figure 6. Function of *Hmgpi* in peri-implantation development. (**A**) Blastocyst outgrowth and alkaline phosphatase (AP) activity in the siHmgpi-injected and siControl-injected embryos, carried out according to a standard procedure (42). Representative images of phase-contrast microscopy for blastocyst outgrowth and fluorescent immunocytochemistry for AP are shown. Scale bar = 100 μM. (**B**) Confocal microscopy images of blastocyst outgrowth for the siHmgpi-injected and siControl-injected embryos, stained with antibodies to Hmgpi and Oct4. Nuclei are shown by DAPI staining. Scale bar = 100 μM. (**C**) Successful rate of blastocyst outgrowth for siHmgpi-injected and siControl-injected embryos. Successful outgrowth in this assay was indicated by the presence of proliferating cells after 6 days in culture. The experiment was repeated four times. (**D**) BrdU incorporation assay for blastocyst outgrowth of the siHmgpi-injected and siControl-injected embryos. Cell proliferation was determined by BrdU incorporation (ICM: arrowhead, trophectodermal cells: arrow). The trophectodermal component contained few cells and BrdU incorporation was confined to the ICM core; however, cell proliferation was reduced in the blastocyst outgrowth of siHmgpi-injected embryos compared with that of the siControl-injected embryos. Nuclei are shown by DAPI staining. Scale bar = 100 μM. (**E**) Immunocytochemistry with an anti-caspase3 antibody in blastocyst outgrowth of the siHmgpi-injected and siControl-injected embryos. Apoptotic cells were not apparent in the blastocyst outgrowth of either injected embryo. Nuclei are shown by DAPI staining. Scale bar = 100 μM. (**F**) Successful rate of siHmgpi-injected and siControl-injected embryo transfer. We transferred 3.5 dpc blastocysts into the uteri of 2.5 dpc pseudopregnant ICR female mice. The pregnant ICR mice were sacrificed on day 12.5 of gestation and the total numbers of implantation sites and of live and dead embryos/fetuses were counted. The experiment was repeated four times.

scription of the 45S precursor of ribosomal RNA (rRNA) by Pol I (24,25). Because the association of UBTF with rRNA genes *in vivo* is not restricted to the promoter and extends across the entire transcribed portion, UBTF promotes the formation of nucleolar organizer regions, indicative of 'open' chromatin (26). Based on the sequence similarity between UBTF and HMGPI, HMGPI might also bind to DNA in a non-specific manner, and modulate chromatin during peri-implantation when dynamic chromatin change is essential.

Alternatively, HMGPI may act as a cytokine during preimplantation development in a similar manner to HMGB1. HMGB proteins are found primarily in the cell nucleus, but also to varying extents in the cytosol (27,28), and have been suggested to shuttle between compartments (17). HMGB1 is indeed passively released from nuclei upon cell death and actively secreted as a cytokine (29), and the addition of recombinant HMGB1 into culture medium enhances *in vitro* development of mouse zygotes to the blastocyst stage in the absence of BSA supplementation (30). Although HMGPI failed to be detected in culture media after *in vitro* culture of preimplantation embryos or ES cells in this study (data not shown), two different modes of Hmgpi action, chromatin modulator and secreted mediator, should be taken into consideration as discussed later.

Role of *Hmgpi* during peri-implantation

The HMGPI protein was first detected in 4-cell embryos and then abundantly expressed in 8-cell embryos, morulae, ICM, trophectoderm and ES cells. Although *Hmgpi* transcription peaked at the 4-cell stage, the most dramatic siRNA effect appeared at the blastocyst and subsequent stages. This discrepancy between temporal expression and phenotype is attributed to three possible mechanisms. First, protein expression is generally delayed from transcription, indicated here by the *Hmgpi* transcripts and HMGPI protein expression peaking at the 4-cell stage and blastocyst stage, respectively. Similarly, *Stella* (31) and *Pms2* (32) are maternal-effect genes, but do not cause developmental loss until later preimplantation stages. A second possibility is the incompleteness of siRNA knockdown. One limitation of such knockdown experiments is the potential variability in levels of silencing of a target gene, which could in turn underlie the observed phenotypic variability in the present study. Embryos with complete suppression of Hmgpi may exhibit developmental arrest at earlier stages (e.g. at the morula stage), while those with less suppression may not display a phenotype until the later stages (e.g. at the implantation stage). Ideally, the suppression level of each embryo could be experimentally analyzed to correlate with the phenotype. The third possibility is spatial translocation of HMGPI protein in the blastocyst cells. The HMGPI expression pattern indicated differential spatial requirements during early embryogenesis, supported by the apparent ability of HMGPI to shuttle between the nucleus and the cytoplasm; the cytoplasmic HMGPI observed from the 4-cell to morula stages and the nuclear HMGPI in blastocysts and ES cells could have different functions. A bipartite nuclear localization signal (NLS) peptide (FKKEKEDFQKKMRQFKK) similar to NLS of HMGN2/HMG-17 (33) is also present in the HMGPI sequence. Thus, the nuclear HMGPI in blastocysts and ES cells might exert a critical transcriptional role to regulate gene expression essential for peri-implantation development. Indeed, the siHmgpi-induced knockdown of *Hmgpi* expression downregulated *Cdx2* in trophectodermal cells and *Oct4* and *Nanog* in ICM cells, with subsequently reduced proliferation of trophectodermal cells and ICM-derived cells during blastocyst outgrowth.

Genes indispensable for derivation of ES cells

Like *Hmgpi*, *Zscan4* is another exclusively zygotic gene not expressed at any other developmental stage (13). *Zscan4* is a putative transcription factor harboring a SCAN domain and zinc finger domains, and transcribed not only in preimplantation embryos but also in ES cells (13). Reduction of *Zscan4* by RNA interference showed a phenotype similar to that induced by *Hmgpi* knockdown: developmental deterioration at the preimplantation stages, especially cleavage pause at 2-cell stage, and failure in blastocyst outgrowth, ES-cell derivation and implantation. Thus, a preimplantation-specific gene expression pattern could indicate a function in ES-cell derivation and/or maintenance. Indeed, *Hmgpi* was also expressed in entire ES colonies, whereas *Zscan4* shows a peculiar mosaic expression pattern in undifferentiated ES cell colonies. Furthermore, the *Hmgpi* gene is highly expressed in ES cells, but not in EC cells; *Hmgpi* is thus eligible as a putative ECAT (ES cell-associated transcript), whose ESTs are overrepresented in cDNA libraries from ES cells compared with those from somatic tissues and other cell lines including EC cells (34). It is also likely that *Hmgpi* is expressed in iPS cells, based on *in silico* analyses of expression profiles [NCBI GEO database, e.g. GSE10806 (35)]. Thus, *Hmgpi* is likely to have a role in maintaining pluripotent cells, since the ECATs such as *Nanog*, *Eras* and *Gdf3* are required for pluripotency and proliferation of ES cells (34,36,37). In the current study, *Hmgpi* was indeed involved in blastocyst outgrowth of ICM cells. On the other hand, several genes including ECAT members have been implicated in trophectodermal development as well as in early embryonic development. Like *Hmgpi* that was expressed in both ICM cells and trophectodermal cells, *Dnmt3l/Ecat7* has a role in embryonic and extra-embryonic tissues in early developmental stages. *DNMT3L* is recruited by *DNMT3A2* to chromatin (38) to function in DNA methylation in ES cells, and defects in maternal *DNMT3L* induce a differentiation defect in the extra-embryonic tissue (39). The reduced CDX2 expression in blastocysts and poor BrdU incorporation during blastocyst outgrowth following siHmgpi knockdown suggested the potential involvement of *Hmgpi* in trophectodermal development.

In summary, *Hmgpi* is required early on in mammalian development to generate healthy blastocysts that implant successfully and produce ES cells. HMGPI translocates into the nucleus from cytoplasm at the blastocyst stage, which is importantly a turning point of early embryonic development when DNA-methylation levels are at their lowest and implantation takes place. The nuclear HMGPI in blastocysts and ES cells is expected to act as a transcription factor to regulate gene expression networks underlying the generation, self-renewal and maintenance of pluripotent cells. Because E7 embryos have already stopped expressing *Hmgpi*, it is likely

that *Hmgpi* stage-specifically regulates a set of genes that drive peri-implantation development. It will be valuable to identify both cofactors that bind HMGPI and recognize specific DNA sequences, as well as genes that are regulated by *Hmgpi* using ES cells. A better understanding of the *Hmgpi* transcriptional network will also improve culture methods for healthy blastocysts and for generating, maintaining and differentiating ES cells.

MATERIALS AND METHODS

Identification of the mouse *Hmgpi* gene by *in silico* analysis

Preimplantation-specific genes were identified based on global gene expression profiling of oocytes and preimplantation embryos (3,40) and expressed sequence tag (EST) frequencies in the Unigene database. SMART (19) was used for domain prediction analysis. Orthologous relationships between HMG family genes were identified from phylogenetic-tree amino acid sequences determined by a sequence distance method and the Neighbor Joining (NJ) algorithm (41) using Vector NTI software (Invitrogen, Carlsbad, CA, USA).

Collection and manipulation of embryos

Six- to 8-week-old B6D2F1 mice were superovulated by injecting 5 IU of pregnant-mare serum gonadotropin (PMS; Calbiochem, La Jolla, CA, USA) followed by 5 IU of human chorionic gonadotropin (HCG; Calbiochem) 48 h later. The Institutional Review Board of the National Research Institute for Child Health and Development, Japan granted ethics approval for embryo collection from the mice. Unfertilized eggs were harvested 18 h after the HCG injection by a standard published method (42), and the cumulus cells were removed by incubation in M2 medium (EmbryoMax M-2 Powdered Mouse Embryo Culture Medium; Millipore, Billerica, MA, USA) supplemented with 300 μg/ml hyaluronidase (Sigma-Aldrich, St Louis, MO, USA). The eggs were then thoroughly washed, selected for good morphology and collected. Fertilized eggs were also harvested from mated superovulated mice in the same way as unfertilized eggs and embryos with two pronuclei (PN) were collected to synchronize *in vitro* embryo development. Fertilized eggs were cultured in synthetic oviductal medium enriched with potassium (EmbryoMax KSOM Powdered Mouse Embryo Culture Medium; Millipore) at 37°C in an atmosphere of 95% air/5% CO_2. Cultured blastocysts were transferred into pseudopregnant recipients as described previously (42). We transferred 3.5 dpc blastocysts into the uteri of 2.5 dpc pseudopregnant ICR female mice. RNA interference experiments were carried out by microinjecting <10 pl (25 ng/μl) of oligonucleotides (siHmgpi and siControl) into the cytoplasm of zygotes. The optimal siRNAs were determined by testing different concentrations (5, 10, 25 and 50 ng/μl) of three siRNAs (PE Applied Biosystems, Foster City, CA, USA), resuspended and diluted with the microinjection buffer (Millipore). Their target sequences are listed in Supplementary Material, Table S3. More than 10 independent experiments were performed to study the effect of *Hmgpi* knockdown on preimplantation development and implantation.

Culture of ES cells and blastocyst outgrowth

A mouse ES cell line (B6/129ter/sv line) was first cultured for two passages on gelatin-coated culture dishes in the presence of leukemia inhibitory factor (LIF) to remove contaminating feeder cells. Cells were then seeded on gelatin-coated 6-well plates at a density of $1–2 \times 10^5$/well ($1–2 \times 10^4$/cm^2) and cultured for 3 days in complete ES medium: KnockOut DMEM (Invitrogen) containing 15% KnockOut Serum Replacement (KSR; Invitrogen), 2000 U/ml ESGRO (mLIF; Chemicon, Temecula, CA, USA), 0.1 mM non-essential amino acids, 2 mM GlutaMax (Invitrogen), 0.1 mM beta-mercaptoethanol (2-ME; Invitrogen) and penicillin/streptomycin (50 U/50 μg/ml; Invitrogen). Blastocyst outgrowth experiments were carried out according to a standard procedure (42). In brief, zona pellucidae of blastocysts at 3.5 dpc were removed using acidic Tyrode's solution (Sigma). The blastocysts were cultured individually in the ES medium on gelatinized chamber slides at 37°C in an atmosphere of 5% CO_2. The cultured cells were examined and photographed daily. Alkaline phosphatase activity was measured using a specific detection kit (Vector Laboratories, CA, USA) after 6 days in culture. Four independent experiments were performed.

Immunostaining of oocytes and preimplantation embryos

Samples were fixed in 4% paraformaldehyde (Wako Pure Chemical, Osaka, Japan) with 0.1% glutaraldehyde (Wako) in phosphate-buffered saline (PBS) for 10 min at room temperature (RT), and then permeabilized with 0.5% Triton X-100 (Sigma) in PBS for 30 min. Immunocytochemical staining was performed by incubating the fixed samples with primary antibodies for 60 min, followed by secondary antibodies for 60 min. A polyclonal antibody to mouse HMGPI was raised in rabbits against three synthesized peptides designed according to sequence specificity, homology between mouse and human HMGPI, antigenicity, hydrophilicity and synthetic suitability [(i) CIQGHHDGAQSSRQDFTD, (ii) CMSMSGG RSSKFGRTEQS, (iii) ESPRTVSSDMKFQGC; Medical & Biological Laboratories Co, Nagoya, Japan). The anti-HMPGI was used at 1:300 dilution, followed by Alexa Fluor 546 goat anti-rabbit IgG (Molecular Probes, Invitrogen) as the secondary antibody. The anti-Histone H2B antibody (Medical & Biological Laboratories Co, Nagoya, Japan) was used at 1:300 dilution as positive control of nuclear staining, followed by Alexa Fluor 488 goat anti-mouse IgG (Molecular Probes, Invitrogen) as the secondary antibody. Blastocysts were immunostained using a monoclonal anti-Oct4 antibody (mouse IgG2b isotype, 200 μg/ml; Santa Cruz Biotechnology, Santa Cruz, CA, USA), rabbit polyclonal anti-Nanog antibody (ReproCELL, Tokyo, Japan), mouse monoclonal anti-Cdx2 antibody (CELL MARQUE, Rocklin, CA, USA), mouse monoclonal anti-BrdU antibody (Santa Cruz) and rabbit monoclonal anti-active caspase 3 (Abcam) antibody, all diluted at 1:50–300. The appropriate secondary antibodies (IgG) were diluted at 1:300 and supplied by Molecular Probes/Invitrogen: goat anti-rabbit IgG conjugated with Alexa Fluor 546 and goat anti-mouse IgG(H + L) conjugated with Alexa Fluor 488. The cellular DNA (nuclei) was stained with 4′,6-diamidino-2-phenylindole (DAPI; Wako; diluted

1:300). The cells were then washed with PBS and viewed by laser confocal microscopy (LSM510, Zeiss). For HMGPI immunostaining, all samples were processed simultaneously. The laser power was adjusted so that the signal intensity was below saturation for the developmental stage that displayed the highest intensity and all subsequent images were scanned at that laser power. This allowed us to compare signal intensities for HMGPI expression at different developmental stages. The other molecules in blastocysts and outgrowth were viewed and imaged as for the HMGPI expression.

Immunocytochemistry of blastocyst outgrowths and ES cells

Cultured ES cells and blastocyst outgrowths were fixed with 4% paraformaldehyde for 10 min at 4°C, treated with 0.1% Triton X-100 (Sigma) in PBS for 15 min at RT, and then incubated for 30 min at RT in protein-blocking solution consisting of PBS supplemented with 5% normal goat serum (Dako, Glostrup, Denmark). The samples were then incubated overnight with the primary antibodies to OCT4, HMGPI, BrdU or active caspase 3 in PBS at 4°C. The cells were then extensively washed in PBS and incubated at RT with Alexa Fluor 488 goat anti-mouse IgG1 (anti-OCT4 and anti-BrdU antibodies, diluted 1:300; Molecular Probes) or Alexa Fluor 546 goat anti-rabbit IgG(H + L) (anti-HMGPI and anti-caspase 3 antibodies, diluted 1:300), and nuclei were counterstained with DAPI for 30 min. To prevent fading, cells were then mounted in Dako fluorescent mounting medium (Dako).

Incorporation of bromodeoxyuridine (BrdU)

E3.5 blastocysts and blastocyst outgrowths were cultured for 16 h in KSOM and ES medium, respectively, supplemented with 10 μM BrdU (Sigma). Samples were then fixed in 4% paraformaldehyde for 20 min, washed in PBS and then treated with 0.5 M HCl for 30 min.

RNA extraction and real-time quantitative reverse transcriptase (qRT)–PCR

Embryos for qRT–PCR analysis were collected at 18 h post-hCG and cultured as described above. They were harvested at 0.5, 1.25, 1.75, 2.25, 2.75 and 3.75 dpc to obtain fertilized eggs 2-cell, 4-cell, 8-cell, morula and blastocyst embryos, respectively. Three subsets of 10 and 50 synchronized and intact embryos were transferred in PBS supplemented with 3 mg/ml polyvinylpyrrolidone (PVP) and stored in liquid nitrogen. Total RNA from 10 and 50 embryos was extracted using the PicoPure RNA Isolation Kit (Arcturus, La Jolla, CA, USA). The reverse transcription reaction, primed with polyA primer, was performed using Superscript III reverse transcriptase (Invitrogen) following the manufacturer's instructions. Total RNA isolated was reverse transcribed in a 20 μl volume. The resulting cDNA was quantified by qRT–PCR analysis using the SYBR Green Realtime PCR Master Mix (Toyobo, Osaka, Japan) and ABI Prism 7700 Sequence Detection System (PE Applied Biosystems) as described previously (43). An amount of cDNA equivalent to 1/2 an embryo was used for each real-time PCR reaction with a minimum of three replicates, with no-RT and no-template controls for each gene. Data were normalized against *H2afz* by the ΔΔCt method (44). PCR primers for the genes of *Hmgpi*, *H2afz* and *Gapdh* were listed in Supplementary Material, Table S4. Calculations were automatically performed by ABI software (Applied BioSystems). For alpha-amanitin studies, fertilized eggs were first harvested at 18 h post-hCG, instead of eggs already advanced to the two-pronucleus stage. After 3 h of incubation, eggs that carried both male and female pronuclei were selected at 21 h post-hCG and randomly assigned to two experimental groups: with and without addition of alpha-amanitin to the culture medium. The eggs were further cultured in KSOM at 37°C in an atmosphere of 5% CO_2 until the specified time point (32, 43 and 54 h post-hCG). Embryos used for alpha-amanitin studies and RNA interference experiments were subjected to qRT–PCR as described for the normal preimplantation embryos.

Immunoblot analysis

Protein samples from embryos were solubilized in Sample Buffer Solution without 2-ME (Nacalai Tesque, Kyoto, Japan), resolved by NuPAGE Novex on Tris-acetate mini gels (Invitrogen), and transferred to Immobilon-P transfer membrane (Millipore). The membrane was soaked in protein blocking solution (Blocking One solution, Nacalai) for 30 min at RT before an overnight incubation at 4°C with primary antibody, also diluted in blocking solution. The membrane was then washed three times with TBST (Tris-buffered saline with 0.1% Tween-20), incubated with a horseradish peroxidase-conjugated secondary antibody (0.04 μg/ml) directed against the primary antibody for 60 min, and washed three times with TBST. The signal was detected by enhanced chemiluminescence (SuperSignal West Dura Extended Duration Substrate, Thermoscientific, Rockford, IL, USA) following the manufacturer's recommendations. The intensity of the band was quantified using NIH Image J software. Briefly, the signal was outlined and the mean intensity and background fluorescence were measured. The specific signal was calculated by dividing the band intensities for HMGPI by those for actin.

Statistical analysis

Differences between groups were evaluated statistically using Student's *t*-test or ANOVA, with *P*-values < 0.05 considered significant.

SUPPLEMENTARY MATERIAL

Supplementary Material is available at *HMG* online.

ACKNOWLEDGEMENTS

The authors would like to thank Dr Takashi Hiiragi for valuable advice and critical reading of the manuscript.

Conflict of Interest statement. The authors declare that there is no conflict of interest that would prejudice the impartiality of the scientific work.

FUNDING

This work was supported, in part, by Grants-in-Aid from the Japan Society for the Promotion of Science (19591911 to T.H., 21390456 to H.A.), by a National Grant-in-Aid from Japanese Ministry of Health, Labor, and Welfare (H21-001, H20-001 to T.H., H18-004 to H.A. and N.K.) and by a Grant-in-Aid from the Yamaguchi- Endocrine Organization to T.H. Funding to pay the Open Access publication charges for this article was provided by Grants-in-Aid for Young Scientists (B) (21791581 to M.Y.).

REFERENCES

1. DePamphilis, M.L., Kaneko, K.J. and Vassilev, A. (2002) Activation of zygotic gene expression in mammals. DePamphilis, M.L. (ed.), *Advances in Developmental Biology and Biochemistry*, Vol. 12, Elsevier Science, B.V.
2. Latham, K.E. and Schultz, R.M. (2001) Embryonic genome activation. *Front. Biosci.*, **6**, D748–D759.
3. Hamatani, T., Carter, M.G., Sharov, A.A. and Ko, M.S. (2004) Dynamics of global gene expression changes during mouse preimplantation development. *Dev. Cell.*, **6**, 117–131.
4. Takahashi, K. and Yamanaka, S. (2006) Induction of pluripotent stem cells from mouse embryonic and adult fibroblast cultures by defined factors. *Cell*, **126**, 663–676.
5. Hamatani, T., Yamada, M., Akutsu, H., Kuji, N., Mochimaru, Y., Takano, M., Toyoda, M., Miyado, K., Umezawa, A. and Yoshimura, Y. (2008) What can we learn from gene expression profiling of mouse oocytes? *Reproduction*, **135**, 581–592.
6. Ko, M.S., Kitchen, J.R., Wang, X., Threat, T.A., Hasegawa, A., Sun, T., Grahovac, M.J., Kargul, G.J., Lim, M.K., Cui, Y. *et al.* (2000) Large-scale cDNA analysis reveals phased gene expression patterns during preimplantation mouse development. *Development*, **127**, 1737–1749.
7. Okazaki, Y., Furuno, M., Kasukawa, T., Adachi, J., Bono, H., Kondo, S., Nikaido, I., Osato, N., Saito, R., Suzuki, H. *et al.* (2002) Analysis of the mouse transcriptome based on functional annotation of 60,770 full-length cDNAs. *Nature*, **420**, 563–573.
8. Solter, D., de Vries, W.N., Evsikov, A.V., Peaston, A.E., Chen, F.H. and Knowles, B.B. (2002) Fertilization and activation of the embryonic genome. Rossant, J. and Tam, P.P.L. (eds), *Mouse Development: Patterning, Morphogenesis, and Organogenesis.*, Academic Press, San Diego, pp. 5–19.
9. Wang, Q.T., Piotrowska, K., Ciemerych, M.A., Milenkovic, L., Scott, M.P., Davis, R.W. and Zernicka-Goetz, M. (2004) A genome-wide study of gene activity reveals developmental signaling pathways in the preimplantation mouse embryo. *Dev. Cell.*, **6**, 133–144.
10. Wang, S., Cowan, C.A., Chipperfield, H. and Powers, R.D. (2005) Gene expression in the preimplantation embryo: in-vitro developmental changes. *Reprod. Biomed. Online*, **10**, 607–616.
11. Zeng, F., Baldwin, D.A. and Schultz, R.M. (2004) Transcript profiling during preimplantation mouse development. *Dev. Biol.*, **272**, 483–496.
12. Choo, K.B., Chen, H.H., Cheng, W.T., Chang, H.S. and Wang, M. (2001) In silico mining of EST databases for novel pre-implantation embryo-specific zinc finger protein genes. *Mol. Reprod. Dev.*, **59**, 249–255.
13. Falco, G., Lee, S.L., Stanghellini, I., Bassey, U.C., Hamatani, T. and Ko, M.S. (2007) Zscan4: a novel gene expressed exclusively in late 2-cell embryos and embryonic stem cells. *Dev. Biol.*, **307**, 539–550.
14. Kanka, J. (2003) Gene expression and chromatin structure in the pre-implantation embryo. *Theriogenology*, **59**, 3–19.
15. Schultz, R.M. and Worrad, D.M. (1995) Role of chromatin structure in zygotic gene activation in the mammalian embryo. *Semin. Cell Biol.*, **6**, 201–208.
16. Thompson, E.M., Legouy, E. and Renard, J.P. (1998) Mouse embryos do not wait for the MBT: chromatin and RNA polymerase remodeling in genome activation at the onset of development. *Dev. Genet.*, **22**, 31–42.
17. Stros, M., Launholt, D. and Grasser, K.D. (2007) The HMG-box: a versatile protein domain occurring in a wide variety of DNA-binding proteins. *Cell. Mol. Life Sci.*, **64**, 2590–2606.
18. Zhang, Q. and Wang, Y. (2008) High mobility group proteins and their post-translational modifications. *Biochim. Biophys. Acta*, **1784**, 1159–1166.
19. Schultz, J., Milpetz, F., Bork, P. and Ponting, C.P. (1998) SMART, a simple modular architecture research tool: identification of signaling domains. *Proc. Natl Acad. Sci. USA*, **95**, 5857–5864.
20. Mamo, S., Gal, A.B., Bodo, S. and Dinnyes, A. (2007) Quantitative evaluation and selection of reference genes in mouse oocytes and embryos cultured in vivo and in vitro. *BMC Dev. Biol.*, **7**, 14.
21. Hock, R., Furusawa, T., Ueda, T. and Bustin, M. (2007) HMG chromosomal proteins in development and disease. *Trends Cell Biol.*, **17**, 72–79.
22. Svarcova, O., Dinnyes, A., Polgar, Z., Bodo, S., Adorjan, M., Meng, Q. and Maddox-Hyttel, P. (2009) Nucleolar re-activation is delayed in mouse embryos cloned from two different cell lines. *Mol. Reprod. Dev.*, **76**, 132–141.
23. Sanij, E., Poortinga, G., Sharkey, K., Hung, S., Holloway, T.P., Quin, J., Robb, E., Wong, L.H., Thomas, W.G., Stefanovsky, V. *et al.* (2008) UBF levels determine the number of active ribosomal RNA genes in mammals. *J. Cell Biol.*, **183**, 1259–1274.
24. Stefanovsky, V.Y., Pelletier, G., Hannan, R., Gagnon-Kugler, T., Rothblum, L.I., Moss, T., Bazett-Jones, D.P. and Crane-Robinson, C. (2001) An immediate response of ribosomal transcription to growth factor stimulation in mammals is mediated by ERK phosphorylation of UBF DNA looping in the RNA polymerase I enhancesome is the result of non-cooperative in-phase bending by two UBF molecules. *Mol. Cell.*, **8**, 1063–1073.
25. Stefanovsky, V.Y., Pelletier, G., Bazett-Jones, D.P., Crane-Robinson, C. and Moss, T. (2001) DNA looping in the RNA polymerase I enhancesome is the result of non-cooperative in-phase bending by two UBF molecules. *Nucleic Acids Res.*, **29**, 3241–3247.
26. Mais, C., Wright, J.E., Prieto, J.L., Raggett, S.L. and McStay, B. (2005) UBF-binding site arrays form pseudo-NORs and sequester the RNA polymerase I transcription machinery. *Genes Dev.*, **19**, 50–64.
27. Falciola, L., Spada, F., Calogero, S., Langst, G., Voit, R., Grummt, I. and Bianchi, M.E. (1997) High mobility group 1 protein is not stably associated with the chromosomes of somatic cells. *J. Cell Biol.*, **137**, 19–26.
28. Bonaldi, T., Talamo, F., Scaffidi, P., Ferrera, D., Porto, A., Bachi, A., Rubartelli, A., Agresti, A. and Bianchi, M.E. (2003) Monocytic cells hyperacetylate chromatin protein HMGB1 to redirect it towards secretion. *EMBO J.*, **22**, 5551–5560.
29. Wang, H., Bloom, O., Zhang, M., Vishnubhakat, J.M., Ombrellino, M., Che, J., Frazier, A., Yang, H., Ivanova, S., Borovikova, L. *et al.* (1999) HMG-1 as a late mediator of endotoxin lethality in mice. *Science*, **285**, 248–251.
30. Cui, X.S., Shen, X.H. and Kim, N.H. (2008) High mobility group box I (HMGB1) is implicated in preimplantation embryo development in the mouse. *Mol. Reprod. Dev.*, **75**, 1290–1299.
31. Payer, B., Saitou, M., Barton, S.C., Thresher, R., Dixon, J.P., Zahn, D., Colledge, W.H., Carlton, M.B., Nakano, T. and Surani, M.A. (2003) Stella is a maternal effect gene required for normal early development in mice. *Curr. Biol.*, **13**, 2110–2117.
32. Gurtu, V.E., Verma, S., Grossmann, A.H., Liskay, R.M., Skarnes, W.C. and Baker, S.M. (2002) Maternal effect for DNA mismatch repair in the mouse. *Genetics*, **160**, 271–277.
33. Hock, R., Scheer, U. and Bustin, M. (1998) Chromosomal proteins HMG-14 and HMG-17 are released from mitotic chromosomes and imported into the nucleus by active transport. *J. Cell Biol.*, **143**, 1427–1436.
34. Mitsui, K., Tokuzawa, Y., Itoh, H., Segawa, K., Murakami, M., Takahashi, K., Maruyama, M., Maeda, M. and Yamanaka, S. (2003) The homeoprotein Nanog is required for maintenance of pluripotency in mouse epiblast and ES cells. *Cell*, **113**, 631–642.
35. Kim, J.B., Zaehres, H., Wu, G., Gentile, L., Ko, K., Sebastiano, V., Arauzo-Bravo, M.J., Ruau, D., Han, D.W., Zenke, M. *et al.* (2008)

Pluripotent stem cells induced from adult neural stem cells by reprogramming with two factors. *Nature*, **454**, 646–650.
36. Levine, A.J. and Brivanlou, A.H. (2006) GDF3, a BMP inhibitor, regulates cell fate in stem cells and early embryos. *Development*, **133**, 209–216.
37. Takahashi, K., Mitsui, K. and Yamanaka, S. (2003) Role of ERas in promoting tumour-like properties in mouse embryonic stem cells. *Nature*, **423**, 541–545.
38. Nimura, K., Ishida, C., Koriyama, H., Hata, K., Yamanaka, S., Li, E., Ura, K. and Kaneda, Y. (2006) Dnmt3a2 targets endogenous Dnmt3L to ES cell chromatin and induces regional DNA methylation. *Genes Cells*, **11**, 1225–1237.
39. Arima, T., Hata, K., Tanaka, S., Kusumi, M., Li, E., Kato, K., Shiota, K., Sasaki, H. and Wake, N. (2006) Loss of the maternal imprint in Dnmt3Lmat-/- mice leads to a differentiation defect in the extraembryonic tissue. *Dev. Biol.*, **297**, 361–373.
40. Pan, H., O'Brien, M.J., Wigglesworth, K., Eppig, J.J. and Schultz, R.M. (2005) Transcript profiling during mouse oocyte development and the effect of gonadotropin priming and development in vitro. *Dev. Biol.*, **286**, 493–506.
41. Saitou, N. and Nei, M. (1987) The neighbor-joining method: a new method for reconstructing phylogenetic trees. *Mol. Biol. Evol.*, **4**, 406–425.
42. Nagy, A., Gertsenstein, M., Vintersten, K. and Behringer, R. (2003) *Manipulating the Mouse Embryo: A Laboratory Manual.*, 3rd edn. Cold Spring Harbor Laboratory.
43. Hamatani, T., Falco, G., Carter, M.G., Akutsu, H., Stagg, C.A., Sharov, A.A., Dudekula, D.B., VanBuren, V. and Ko, M.S. (2004) Age-associated alteration of gene expression patterns in mouse oocytes. *Hum. Mol. Genet.*, **13**, 2263–2278.
44. Falco, G., Stanghellini, I. and Ko, M.S. (2006) Use of Chuk as an internal standard suitable for quantitative RT-PCR in mouse preimplantation embryos. *Reprod. Biomed. Online*, **13**, 394–403.